High Efficiency SiC Traction Inverter for Electric Vehicle Applications

Jianglin Zhu, Hyeokjin Kim, Hua Chen,
Robert Erickson, Dragan Maksimović
Department of Electrical, Computer and Energy Engineering
University of Colorado Boulder
Boulder, Colorado, 80309

Abstract

Silicon Carbide (SiC) MOSFETs, which offer substantial improvements in the device figure of merit, are investigated as alternatives to silicon IGBTs in electric vehicle (EV) drivetrain applications. However, effectiveness of device replacements must be evaluated in the context of system performance, including impact on system efficiency, power density, and thermal management requirements over standard drive cycles. This paper is focused on modeling, design, implementation, and experiment results for a 30 kW rated SiC inverter achieving 99.5% peak efficiency, and high power density (15 kW/L), including cooling plate, drivers and controller. Based on an experimentally calibrated loss model, a quantitative comparison is made between the performance of the SiC MOSFET based inverter and a conventional state-of-art IGBT based inverter system in standard EPA driving cycles (UDDS, HWFET and US06). The results demonstrate that the SiC based inverter has about 3.5x higher Q factor and 3x lower peak loss in the combined (CAFE) drive cycle, together with 2x smaller semiconductor die area.

Index Terms — electric vehicle, traction inverter, SiC MOSFET, EPA drive cycle, loss modeling

I. Introduction

This paper considers the xEV drivetrain architecture shown in Fig. 1, which includes a battery pack, a boost dc-dc converter, a traction inverter, and an ac machine. The power electronics performance is directly related to the vehicle overall drivetrain efficiency and cost. Conventionally, drivetrain power electronics has been based on silicon IGBTs, with switching speed and reverse recovery of silicon junction diodes limiting the performance [1]. SiC MOSFETs offer improved device figure of merit at comparable voltage ratings [2], which opens opportunities to overcome limitations in terms of efficiency and power density [3]. System level benefits, however, require a more detailed investigation, taking into account operation over wide ranges of voltages and power levels associated with typical drive cycles. In this paper, a 30 kW three-phase traction inverter using 1200V SiC-MOSFET devices is described and test results are reported. High efficiency (peak 99.5 %) is verified by experiments. Based on an experimentally calibrated loss model, a quantitative comparison is then made against a state-of-the-art silicon IGBT-based inverter in standard driving cycles, demonstrating system-level benefits of the SiC-based inverter in terms of efficiency and power density.

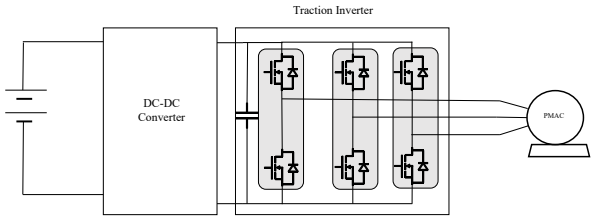

Fig. 1. Drivetrain architecture incorporating a battery pack, a dc-dc converter, a traction inverter, and an ac machine.

II. Traction Inverter Specifications and Design

Specifications for a standard 2-level three phase inverter in Fig. 1 are listed in Table I. For performance comparison, two inverters are considered, one based on 1200V SiC-MOSFETs and the other one based on state-of-the-art IGBTs, as summarized in Table II.

TABLE I
Traction inverter specifications

Input Bus Voltage	250 - 800V
Rated Power	30kW
Maximum Current per Phase	105A
Maximum Modulation Frequency	1kHz

Note that the overall die size in the SiC-MOSFET design is about one half of the overall die size in the IGBT design. Furthermore, the SiC-MOSFET inverter is designed to operate at two times higher switching frequency (20 kHz) compared to the IGBT inverter (10 kHz). Higher switching frequency is generally favorable because it results in reduced THD of the machine current at high RPM, and a higher upper limit for the current control loop bandwidth [4]. However, the impact on the size is limited by the fact that the minimum required bus capacitance volume remains the same between the two inverter designs. This is because the capacitor volume

978-1-5386-1180-7/18/$31.00 ©2018 IEEE

is largely determined by the RMS current rating, which is not related to the switching frequency but rather the power factor of the machine and the modulation index [5].

III. SiC inverter loss model calibrated by experimental results

An accurate loss model is critical to reliably compare the performance of the two inverters described above. To this end, a comprehensive loss model is developed for the SiC inverter, and is experimentally calibrated and/or validated over a wide range of input voltages and output currents, as detailed in this section. A similar loss model is also developed for the IGBT inverter.

A. SiC loss model

Piecewise linear (PWL) model [6] considering nonlinear device capacitances [7] is employed in switching loss calculations. An advantage of the PWL switching loss model is that it combines device datasheet parameters and results obtained by relatively simple test experiments. The developed PWL switching loss model is based on the following assumptions:

- The switching loss is negligible when a switching device is operated under zero-voltage switching (ZVS) conditions.
- Ringing losses due to parasitic inductance during switching transition are not considered.

Based on the PWL switching loss model, switching energy can be calculated and then averaged over the entire period using

$$P_{switching} = f_{line} \sum_{n=0}^{N} E_{tot}(n),\ N = \lceil \frac{f_{sw}}{f_{line}} \rceil \tag{1}$$

In addition, the conduction loss can be expressed as

$$P_{conduction} = R_{DS} {I_{RMS}}^2 \tag{2}$$

where R_{DS} is the MOSFET on-state resistance and I_{RMS} is the device RMS current, f_{sw} and f_{line} are the switching frequency and the modulation (line) frequency, respectively, and $E_{tot}(n)$ is the total switching energy at the n^{th} switching event within a line cycle.

B. SiC inverter experimental results

To validate the loss model over wide operating conditions, a prototype SiC inverter is built, achieving peak efficiency of 99.5% at 15 kW and a volumetric power density of 15 kW/L, as shown in Fig. 2. The loss of the inverter is a function of three independent variables: input voltage V_{in}, output RMS current I_{rms}, and switching frequency f_{sw}. To account for nonidealities such as circuit parasitics and temperature variations, both the conduction loss and the switching loss model must be experimentally validated and calibrated. Because only the switching loss is proportional to switching frequency, the actual switching energy can be found as

$$E_{sw} = \frac{\partial P_{tot}}{\partial f_{sw}} \approx \frac{\Delta P_{tot}}{\Delta f_{sw}} \tag{3}$$

The switching loss can be calculated using

$$P_{switching} = E_{sw} f_{sw} \tag{4}$$

and the conduction loss can then be separated from the total measured loss:

$$P_{conduction} = P_{tot} - P_{switching} \tag{5}$$

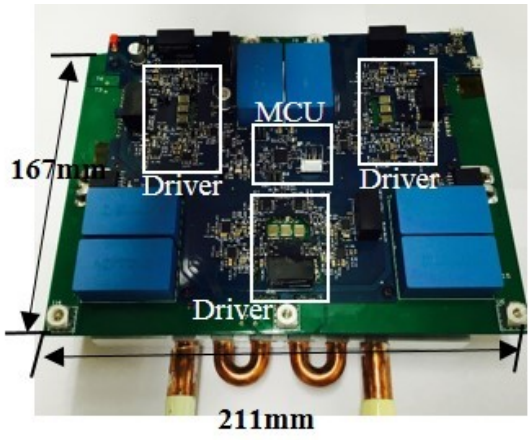

Fig. 2. SiC inverter prototype (211 mm (L) * 167 mm (W) * 55 mm (H)) having 15 kW/L power density, including cooling plate, drivers and controller.

A Y-connected resistive load in series with filter inductors is used in experiments, so that a wide range of input voltage and output current can be easily attained at different switching frequencies. The total loss P_{tot} is measured at each operating point. The equipment used in the experiments is listed in Table III, and the power measurements are calibrated using a calorimetric method assuring a dc error of 0.1 %.

After the calibration, Fig. 3 shows the predicted and measured efficiency results plotted against output power. A comparison of modeled and measured conduction and switching losses is shown in Fig. 4, where a good agreement between the loss model and the experimental results can be observed. In particular, at $V_{in} = 654$ V, $I_{rms} = 22$ A, $P_{out} = 15.7$ kW, the SiC inverter achieves a peak efficiency of 99.5%.

To further validate the model described above, the inverter losses are measured in the case of driving an ac machine with approximately sinusoidal current waveforms. In this experiment, a Parker GVM210 100G Surface Mount Permanent Magnet Synchronous Machine (SMPMSM) is used as the traction motor, and another GVM210 100Q PMSM is used as the load motor to deliver power to a resistor bank (rated at 6 kW). The traction motor is controlled to regulate the rotor speed, while the resistor banks are adjusted to reach a desired torque at steady state. The motor operating waveforms are shown in Fig. 5.

TABLE II
PARAMETERS OF SIC-BASED AND IGBT-BASED TRACTION INVERTERS

	1200V SiC MOSFET	1200V Si IGBT
Device	Transistor: Cree C2M-1200-0025B Diode: CPW5-1200-Z050B	Transistor: Infineon IKW40T120 Diode: SIDC23D120H8
Total Die Area[mm2]	600	1155
Die Per Switch	2	3
Switching Frequency[kHz]	20	10
Bus Capacitance[uF]	28	28

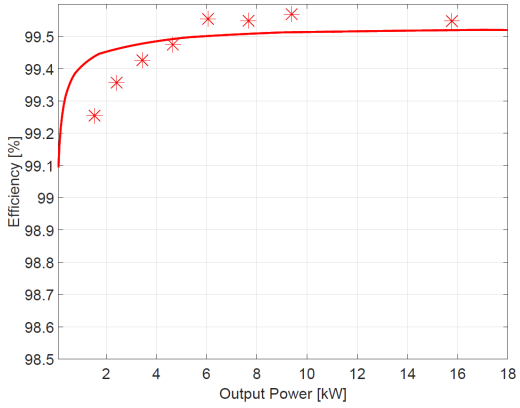

Fig. 3. Measured efficiency points and modeled efficiency (line) as functions of output power with resistive load. Tested voltage range: 200V-680V

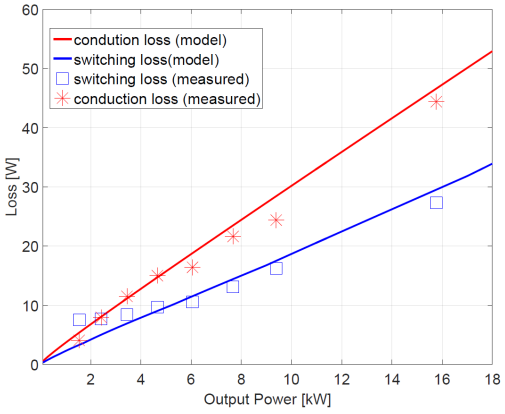

Fig. 4. Loss breakdown as a function of output power at the operating points shown in Fig 3: measured points, and loss model based results (lines).

TABLE III
TEST SETUP FOR EFFICIENCY MEASUREMENTS

Input voltage	Tektronix DMM 4050 (6.5 digit Multimeter)
Input current	LEM IST UltraStab current sensor feed into Tektronix DMM 4050 (6.5 digit Multimeter)
Output power	Yokogawa WT3000 Precision Power Analyzer

The experimental procedure is as follows: first, the load bank is set to a certain value and the bus voltage is kept constant. The traction motor is then regulated at different speeds all the way up to its maximum allowed value. Several sets of data (including ac RMS current for torque estimation, speed and efficiency) are taken and averaged during steady state operation. The results are shown in the speed/torque plane in Fig. 6 for 500 V input voltage. The machine is operated under $i_d = 0$ (i.e. constant torque angle) and the machine power factor at each operating point can be estimated. Good agreement between model predictions and measured values can be observed in Fig. 6, further validating the loss model. It can be observed how inverter efficiency varies with operating point of the motor, with higher efficiency at intermediate speed/torque combinations, and lower efficiency along the two axes where high-torque or high-speed operation contributes to increased conduction or switching losses, respectively, especially at lower power levels.

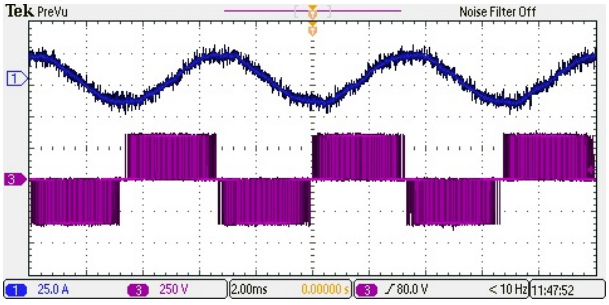

Fig. 5. Traction motor operating waveforms: motor current (CH1) and motor terminal voltage (CH3) at $V_{in} = 350$ V.

C. IGBT loss model

Conventional EV traction inverters are typically based on 1200 V Si-IGBT devices. For a selected IGBT [8], loss model parameters are given in Table II. The conduction loss is calculated by:

$$P_{conduction} = V_{ces} I_{ce} + R_q I_{ce}^2 \tag{6}$$

and the switching loss is approximated as:

$$P_{switching} = f_{sw}(K_{sw-on} I_{ce}^{a_{on}} V_{ce}^{b_{on}} + K_{sw-off} I_{ce}^{a_{off}} V_{ce}^{b_{off}}) \tag{7}$$

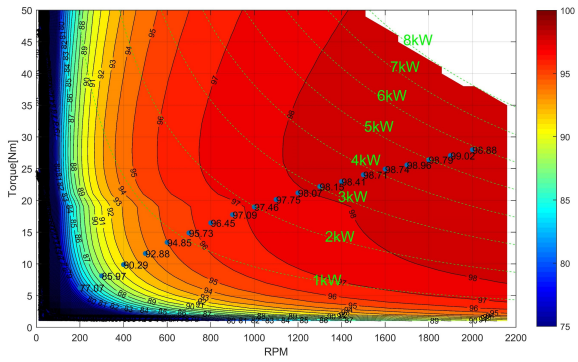

Fig. 6. Inverter efficiency contours at $V_{in} = 500$ V in the motor torque versus speed plane. Results are shown based on the loss model, and based on experiments (scattered blue dots with efficiency numbers annotated)

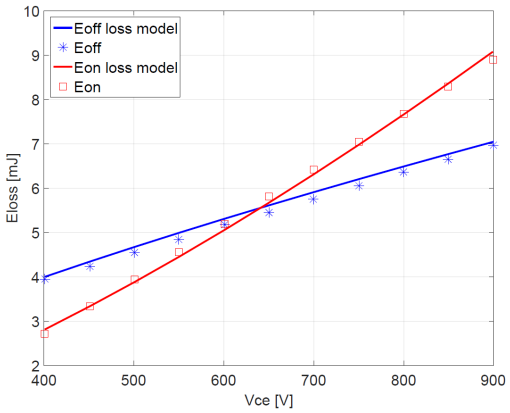

Fig. 7. IGBT modeled and measured switching energy (datasheet) at $I_{ce} = 40$ A as functions of dc bus voltage

where V_{ce} and I_{ce} are blocking voltage and conducting current, and all other parameters can be found by curve fitting using the manufacture's datasheet as listed in Table IV [8]. A comparison to datasheet-based measured losses is provided in Figs. 8 and 7. Note that the IGBT performance is substantially limited by diode reverse recovery and current "tailing" during turn off. The datasheet based loss data incorporate both mechanisms, assuming a silicon anti-parallel diode. A combination of IGBT's with SiC anti-parallel diodes may offer another alternative in cost versus performance trade-off considerations.

TABLE IV
1200V IGBT LOSS MODEL PARAMETERS

K_{sw-on}	1.637×10^{-12}
a_{on}	1.536
b_{on}	1.45
K_{sw-off}	1.687×10^{-6}
a_{off}	0.9693
b_{off}	0.7
V_{ces}	0.9V
R_{ce}	$29.5 \times 10^{-3}\Omega$

IV. Drive Cycle Performance Comparison

This sections provides a system level comparison of SiC and IGBT based inverter performance in various standard EPA driving cycles using the loss models described above. To evaluate the performance of the two inverters over a dynamic driving cycle, all operating points must be taken account. However, a brute force loss calculation at every operating point takes large amount of computational effort. To decrease computation power without losing fidelity, this evaluation task is divided into two steps: first, operating points are extracted from a large system simulation with average models and data (inverter voltage, current) are then interpolated at the switching

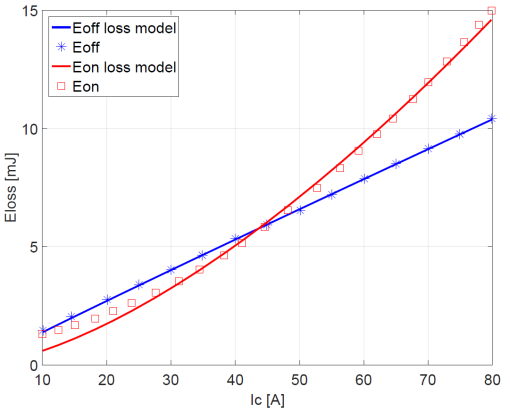

Fig. 8. IGBT modeled and measured switching energy (datasheet) at $V_{ce} = 600$ V as functions of output current

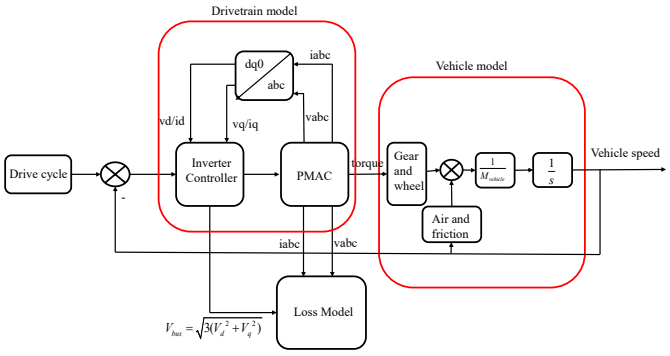

Fig. 9. System simulation model including the drivetrain, and a complete vehicle model

period resolution for loss calculations. The system simulation diagram is shown in Fig. 9.

The full vehicle simulation takes into account the inverter motor drive and electric machine model, gearbox, environmental factors such as air drag and rolling resistance. In order to follow the speed profile defined by the drive cycle, the vehicle speed is regulated by a system controller issuing torque command to the motor controller, while the inverter controller generates a bus voltage command to the boost dc-dc converter, to adjust the input input dc bus voltage as necessary for the given speed [9]. The model assumes the following:

- A Surface Mount PMSM is assumed for the machine model, and constant torque angle ($i_d = 0$) controller incorporating flux weakening operation at high speed operation is used for the inverter controller [10] [11].
- The vehicle system is capable of regenerative braking.
- The peak power of the drivetrain is scaled down to 30 kW, to match the ratings of the considered SiC and IGBT inverters.

As an example, simulation results with active bus voltage control for the US06 drive cycle are shown in Fig. 10. One may note that it is assumed that the system reaches 90 % of peak power during the aggressive US06 drive cycle, which includes frequent acceleration/deceleration as well as high speed cruising segments. However, as seen from the histogram of the operating points in Fig. 11, where a 1D probability density function (pdf) is also plotted for bus voltage and power, most of the operating points are below 30% peak power, which suggests that light load instead of peak power efficiency is more critical for overall system performance [12]. For comparison, only the operating points around 20% peak power are selected, and losses for IGBT and SiC MOSFET based inverters are plotted against the bus voltage in Fig. 12. It can be seen that IGBT exhibits more than 2x higher peak loss due to high current at low bus voltage and about 3x higher loss in the high voltage region.

In the comparison of inverter performance over drive cycles, the inverter quality factor Q is also evaluated. The average efficiency and the quality factor Q are defined as follows:

$$Q = \frac{\int |P_{out}| dt}{\int P_{loss} dt} \tag{8}$$

$$\eta_{avg} = \frac{Q}{Q+1} = \frac{\int |P_{out}| dt}{\int P_{loss} dt + \int |P_{out}| dt} \tag{9}$$

Quality factor Q is an important performance metric because it signifies a trade-off between output power and losses, and therefore thermal management requirements. For a system with higher quality factor, less heat is dissipated per unit output power; on the other hand, if heat dissipation and thermal management remain the same, higher Q implies that more power can be processed [12].

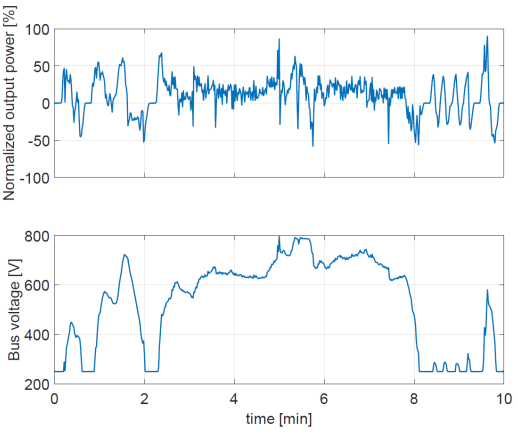

Fig. 10. Normalized power and bus voltage in US06 drive cycle in a system with active bus voltage regulation.

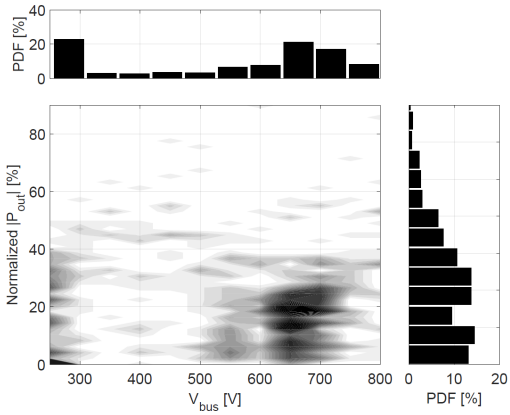

Fig. 11. Histogram of inverter operating points in US06 drive cycle in a system with active bus voltage regulation.

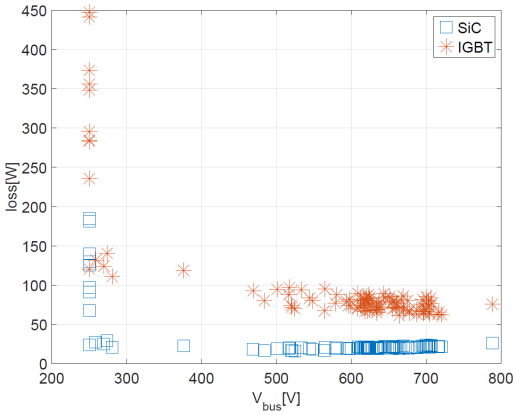

Fig. 12. Loss comparison for IGBT and SiC MOSFET based inverters at 20% peak power in US06 drive cycle

TABLE V
SIMULATED AVERAGE EFFICIENCY AND INVERTER QUALITY FACTOR Q EVALUATED OVER VARIOUS DRIVE CYCLES

	1200V SiC V_{bus} variable	1200V IGBT V_{bus} variable	1200V SiC V_{bus} =800V	1200V IGBT V_{bus} =800V
UDDS avg. efficiency	99.49	97.59	98.7	95.96
/Quality factor	195	40	76	24
HWFET avg. efficiency	99.54	98.68	99.31	98.4
/Quality factor	216	75	144	61
US06 avg. efficiency	99.54	98.07	99.48	97.87
/Quality factor	216	51	191	46
CAFE avg. efficiency	99.51	98.34	99.07	97.59
/Quality factor	204	59	107	41
Peak loss [W]	151	461	170	780
Peak power [kW]	27	27	27	27

The average efficiency and quality factor results for different drive cycles including combined CAFE (Corporate Average Fuel Economy) are presented for comparison in Table V. Two major advantages of SiC traction inverters over IGBT inverters can be deduced from this comparison:

- Overall drive cycle efficiency is improved by about 1% in combined CAFE and 2% in urban driving situations (using variable dc bus voltage approach), which is equivalent to 3.5x and 5x improvements of Q factor, respectively.
- Peak loss for the SiC inverter is 3 times lower on average which also implies reduced thermal management requirements, and opportunities for higher overall power density.

It is also of interest to mention that using active bus voltage regulation by the boost converter the average loss is reduced by about 2x in both IGBT and SiC cases in the urban driving cycle. This is due to the reduction of switching losses, which is the dominating loss mechanism at low speed and low power operation typical for urban driving profiles.

V. CONCLUSIONS

This work presents design and experimental results for a SiC inverter for EV applications, achieving 15 kW/L volumetric density and 99.5% peak efficiency. A comprehensive loss model is developed and calibrated by experiments on a prototype SiC inverter. The loss model is used to perform system level simulations and evaluate the impact of SiC inverter in comparison to a standard IGBT based inverter over various drive cycles. Vehicle system simulations show about 2x reduction in die size, 3x reduction in peak loss, and 3.5x improvement of Q factor compared with IGBT inverter design for different standard driving cycles. In addition, it is shown that active dc bus voltage regulation approach results in about 2x average loss reduction in urban driving profiles.

ACKNOWLEDGEMENT

The information, data, or work presented herein was funded in part by the Office of Energy Efficiency and Renewable Energy (EERE), U.S. Department of Energy, under Award Number DE-EE0006921.

REFERENCES

[1] T. Burress, "Evaluation of the 2010 Toyota Prius hybrid synergy drive system," Oak Ridge National Laboratory (ORNL); Power Electronics and Electric Machinery Research Facility, Technical Report ORNL/TM-2010/253.

[2] A. Hefner, S.-H. Ryu, B. Hull, D. Berning, C. Hood, J. M. Ortiz-Rodriguez, A. Rivera-Lopez, T. Duong, A. Akuffo, and M. Hernandez-Mora, "Recent advances in high-voltage, high-frequency silicon-carbide power devices," in *Industry Applications Conference, 2006. 41st IAS Annual Meeting. Conference Record of the 2006 IEEE*, vol. 1. IEEE, 2006, pp. 330–337.

[3] K. Olejniczak, T. Flint, D. Simco, S. Storkov, B. McGee, R. Shaw, B. Passmore, K. George, A. Curbow, and T. McNutt, "A compact 110 kva, 140 c ambient, 105 c liquid cooled, all-sic inverter for electric vehicle traction drives," in *Applied Power Electronics Conference and Exposition (APEC), 2017 IEEE*. IEEE, 2017, pp. 735–742.

[4] Y. Li, D. Han, and B. Sarlioglu, "Design of high-speed machines using silicon-carbide based inverters," in *Energy Conversion Congress and Exposition (ECCE), 2015 IEEE*. IEEE, 2015, pp. 3895–3900.

[5] H. Wen, W. Xiao, X. Wen, and P. Armstrong, "Analysis and evaluation of dc-link capacitors for high-power-density electric vehicle drive systems," *IEEE Transactions on Vehicular Technology*, vol. 61, no. 7, pp. 2950–2964, 2012.

[6] R. W. Erickson and D. Maksimovic, *Fundamentals of Power Electronics*. Springer, 2001.

[7] H. Kim, H. Chen, D. Maksimovic, and R. Erickson, "Design of a high efficiency 30 kw boost composite converter," in *Energy Conversion Congress and Exposition (ECCE), 2015 IEEE*, Sept 2015, pp. 4243 – 4250.

[8] Infineon, "Low Loss DuoPack : IGBT in TrenchStop and Fieldstop technology with soft, fast recovery anti-parallel Emitter Controlled HE diode," https://infineon.com, 2013, [Online].

[9] H. Kim, H. Chen, J. Zhu, D. Maksimovic, and R. Erickson, "Impact of 1.2kv sic-mosfet ev traction inverter on urban driving," in *Workshop on Wide Bandgap Power Devices and Applications (WiPDA), 2016 IEEE*, November 2016.

[10] S.-K. Sul, *Control of electric machine drive systems*. John Wiley & Sons, 2011, vol. 88.

[11] T.-S. Kwon, G.-Y. Choi, M.-S. Kwak, and S.-K. Sul, "Novel flux-weakening control of an ipmsm for quasi-six-step operation," *IEEE Transactions on Industry Applications*, vol. 44, no. 6, pp. 1722–1731, 2008.

[12] H. Chen, H. Kim, R. Erickson, and D. Maksimović, "Electrified automotive powertrain architecture using composite dc-dc converters," *IEEE Transactions on Power Electronics*, vol. 32, no. 1, pp. 98–116, Jan 2017.